RSC Advances

PAPER

View Article Online
View Journal | View Issue

Cite this: *RSC Adv.*, 2022, **12**, 15479

Fluvirucins B_7–B_{10}, new antifungal macrolactams from a marine-derived *Nonomuraea* sp. MYH522†

Hai Yu,[a] Shuo Chen,[a] Hongji Li,[a] Ruina Wang,[a] Yuanying Jiang,[b] Lan Yan*[a] and Peng Sun*[ab]

Received 16th March 2022
Accepted 11th May 2022

DOI: 10.1039/d2ra01701f

rsc.li/rsc-advances

Marine rare actinomycetes are an important source of secondary metabolites. From a marine-derived actinomycete *Nonomuraea* sp. MYH522, four new macrolactams, fluvirucins B_7–B_{10}, together with known fluvirucin B_6 were isolated. Their structures were determined based on comprehensive analysis of HRESIMS and NMR spectroscopic data as well as by comparing ^{13}C NMR resonances and optical rotation values with those for related congeners. Fluvirucins are characterized by a 14-membered macrolactam attached by an aminosugar moiety. The discovery of fluvirucins B_6–B_{10} enriched the *N*-acetylated derivatives of fluvirucins. The diverse alkyl substituents at C-2 and C-6 implied substrate promiscuity in fluvirucin polyketide biosynthesis. These compounds didn't exhibit any antibacterial or antifungal activities when used alone, which suggested the importance of the free amino group in the antimicrobial activity of fluvirucins. However, fluvirucins B_6, B_9, and B_{10} showed synergistic antifungal activity with fluconazole against fluconazole-resistant isolates of *Candida albicans*.

Introduction

Actinomycetes are characterized as one of the most important microorganisms for producing therapeutic agents in treating infections, pathogens, and cancer.[1] Due to the decrease in discovering new chemical scaffolds, more attention has been drawn to rare actinomycetes or actinomycetes from previously underexplored environments. Marine actinomycetes are found to be a noteworthy source of new bioactive molecules.[2–4] Moreover, rare actinomycetes, which are poorly assessed in contrast to the genus *Streptomyces*, are capable of producing a large number of new secondary metabolites.[5–7]

Fluvirucins are a group of 14-membered macrolactams particularly produced by rare actinomycetes such as the genera of *Actinomadura*, *Nonomuraea*, and *Nocardiopsis*. It should be noted that numerous species of *Actinomadura* were reclassified as *Nonomuraea*.[8] Since the first member Sch 38516 discovered in 1990, twenty fluvirucins have been reported.[9–17] Fluvirucins are shown with various biological properties, *i.e.*, antifungal,[9,14,15] antibacterial,[18–20] antiviral,[10,20,21] and anthelmintic[16,17] activities. The unique structure and the bioactivity of fluvirucins have also attracted attentions of chemists for total synthesis.[22–24]

During our ongoing investigation on new secondary metabolites from marine organisms,[25–27] we encountered a rare actinomycete *Nonomuraea* sp. MYH522, which was isolated from a marine sponge in South China Sea. Chemical investigation of this strain led to the discovery of known fluvirucin B_6 (**1**) together with four new analogs fluvirucins B_7–B_{10} (**2–5**) (Fig. 1). Herein, we reported the isolation, structure elucidation, and biological evaluation of these compounds.

Results

16S rDNA gene sequence and phylogenetic analysis

The 16S rDNA gene of strain MYH522 was amplified by PCR to obtain a 1450 bp sequence with NCBI GenBank accession number of NR117924.1. According to the results of nucleotide BLAST, MYH522 showed the highest sequence similarity to *Nonomuraea jabiensis* A4036 (99.24%). The related reference strains were used to multiple sequence alignment and

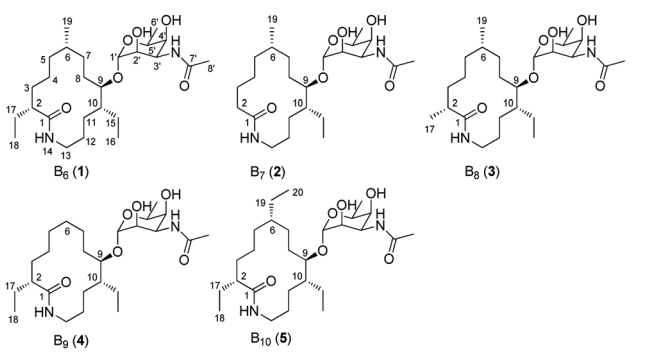

Fig. 1 Structures of fluvirucins B_6–B_{10} (**1–5**).

[a]*School of Pharmacy, Naval Medical University, 325 Guo-He Road, Shanghai 200433, People's Republic of China. E-mail: sunpeng78@126.com; ylansmmu@sina.com*
[b]*Tongji University School of Medicine, 1239 Siping Road, Shanghai, People's Republic of China*

† Electronic supplementary information (ESI) available: Tables S1, S2 and Fig. S1, S2–S5 (MS and NMR spectra of **2–5**). See https://doi.org/10.1039/d2ra01701f

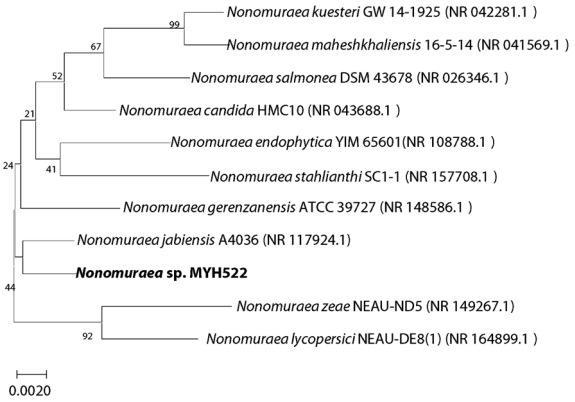

Fig. 2 Neighbor-joining phylogenetic tree of strain MYH522.

phylogenetic analysis based on a neighbor-joining method *via* MEGA7. In the neighbor-joining tree, strain MYH522 fell into the cluster of the genus *Nonomuraea* (Fig. 2). Thus, the strain was notated as *Nonomuraea* sp. MYH522.

Isolation and structural identification

The MYH522 strain was cultivated with 18 L fermentation broth and extracted with ethyl acetate (EtOAc). The extract was fractionated successively by column chromatography (CC) on silica gel, Sephadex LH-20, and RP-HPLC to produce a group of macrolactams. The major constituent was readily determined to be fluvirucin B_6 (**1**) by comparison of ^{1}H and ^{13}C NMR data with those reported.[18] Besides, four new analogs named fluvirucins B_7–B_{10} (**2–5**) were co-isolated. The new compounds were subjected to structure elucidation by a set of spectroscopic experiments.

Fluvirucin B_7 (**2**) was obtained as an amorphous powder. The molecular formula was determined as $C_{24}H_{44}N_2O_6$ by the HRESIMS ion at *m*/*z* 457.3287 $[M + H]^+$ (calcd 457.3278 for $C_{24}H_{45}N_2O_6$), which required four degrees of unsaturations. The IR spectrum of **2** displayed amide absorptions at 3302 cm^{-1} and 1643 cm^{-1}. The structure of **2** was fully assigned by comparision with those of **1** and by further analyses of the 1D and 2D NMR data.[18] The ^{1}H spectrum displayed four methyl groups shown as one methyl singlet, one methyl triplet, and two methyl doublets, which were one methyl triplet less than those of **1**. The ^{13}C NMR and DEPT spectra indicated 24 signals that corresponded to 2 sp^2 (2 C=O) and 22 sp^3 carbon atoms (4 CH_3, 10 CH_2, 3 CH, 4 OCH, and 1 OCO), accounting for two double bond equivalents (DBEs) (Tables 1 and 2). The remaining unsaturations were attributed to two cycles in the structure. The *O*-bearing methine protons resonating between δ_H 3.56 and δ_H 4.86 in conjunction with an acetal carbon (δ_C 99.1, C-1′, CH) suggested the presence of a sugar unit. Analysis of COSY spectrum delineated a long proton spin system of H_2-2/H_2-3/H_2-4/H_2-5/H-6/H_2-7/H_2-8/H-9/H-10/H_2-11/H_2-12/H_2-13, H-6/H_3-19, and H-10/H_2-15/H_3-16 (Fig. 3). The HMBC correlations from H_2-2 (δ_H 2.18, 2.27) and H_2-13 (δ_H 3.20, 3.35) to C-1 (δ_C 176.1, C) connected the long COSY fragment and permitted the establishment of a 14-membered macrolactam skeleton. The HMBC cross-peaks from a methyl doublet (δ_H 0.92, H_3-19) to C-5 (δ_C 34.2, CH_2), C-6 (δ_C 32.4, CH), and C-7 (δ_C 25.7, CH_2) allowed the assignment of a methyl group at C-6. The methyl triplet (δ_H 0.90, H_3-16) suggested the presence of an ethyl group, which was positioned at C-10 based on the HMBC correlations from H_3-16 to C-15 (δ_C 22.8, CH_2) and C-10 (δ_C 41.8, CH).

Table 1 ^{13}C NMR spectroscopic data for **2–5** (in CD_3OD, 150 MHz)

No.	2	3	4	5
1	176.1, C	179.7, C	178.9, C	178.9, C
2	36.2, CH_2	43.0, CH	50.9, CH	51.2, CH
3	26.5, CH_2	36.2, CH_2	34.1, CH_2	34.6, CH_2
4	26.3, CH_2	26.1, CH_2	26.5, CH_2	26.3, CH_2
5	34.2, CH_2	35.2, CH_2	27.9, CH_2	33.4, CH_2
6	32.4, CH	32.4, CH	27.8, CH_2	39.8, CH
7	25.7, CH_2	26.1, CH_2	27.2, CH_2	23.2, CH_2
8	21.9, CH_2	22.8, CH_2	20.0, CH_2	22.6, CH_2
9	78.5, CH	78.7, CH	78.4, CH	78.5, CH
10	41.8, CH	42.3, CH	42.3, CH	42.0, CH
11	26.9, CH_2	26.3, CH_2	26.2, CH_2	26.3, CH_2
12	25.8, CH_2	28.5, CH_2	28.6, CH_2	28.7, CH_2
13	39.7, CH_2	39.8, CH_2	39.7, CH_2	39.7, CH_2
15	22.8, CH_2	22.3, CH_2	22.2, CH_2	22.0, CH_2
16	10.3, CH_3	9.4, CH_3	9.3, CH_3	9.2, CH_3
17		18.9, CH_3	27.7, CH_2	27.5, CH_2
18			12.4, CH_3	12.4, CH_3
19	20.9, CH_3	20.9, CH_3		28.2, CH_2
20				12.8, CH_3
1′	99.1, CH	99.4, CH	99.2, CH	99.3, CH
2′	71.1, CH	71.2, CH	71.1, CH	71.2, CH
3′	49.6, CH	49.6, CH	48.8, CH	48.8, CH
4′	72.2, CH	72.3, CH	72.2, CH	72.2, CH
5′	68.8, CH	68.8, CH	68.8, CH	68.8, CH
6′	17.0, CH_3	17.0, CH_3	17.1, CH_3	17.0, CH_3
7′	173.0, C	173.0, C	173.0, C	173.0, C
8′	22.6, CH_3	22.7, CH_3	22.7, CH_3	22.7, CH_3

The second fragment was interpreted starting from another proton sequence of H-1′/H-2′/H-3′/H-4′/H-5′/H_3-6′ deduced by COSY spectrum. The HMBC correlations from H-1′ to C-5′, from H-2′ and H-4′ to C-3′ (δ_C 49.6, CH), and from H_3-6′ to C-4′ and C-5′ suggested an amino sugar. An acetyl group (δ_H 2.03 H_3-8′; δ_C 22.6 C-8′ CH_3, 173.0 C-7′, C) was substituted at C-3′ NH based on the HMBC correlations from H-3′ (δ_H 4.14) and H_3-8′ to C-7′ and the diagnostic long-range HMBC correlation from H_3-8′ to C-3′. The relative configuration of amino sugar was determined by analysis of coupling constants and NOESY experiment. The obvious NOE correlation of H-3′/H-5′ indicated they were axial protons and in *syn* relationship (Fig. S1†). The anomeric proton (δ_H 4.86, d, J = 1.5) and carbon are resonated at deshielding region indicating an α-pyranoside configuration and an equatorial orientation of H-1′,[10] which was suggested by the absence of NOE correlations of either H-1′/H-3′ or H-1′/H-5′. The small coupling constants of $^3J_{H\text{-}2',H\text{-}3'}$ (3.0) and $^3J_{H\text{-}3',H\text{-}4'}$ (3.0) indicated that both H-2′ and H-4′ were equatorially orientated. The amino sugar was then determined to be *N*-acetyl-4-*epi*-mycosamine. Finally, a HMBC correlation from H-1′ to C-9 (δ_C 78.5, CH) suggested the connectivity of two fragments, completing the structure assignment of **2**.

Table 2 ^{1}H NMR spectroscopic data for **2–5** (in CD_3OD, 600 MHz)

No.	2	3	4	5
2	2.27, m; 2.18, m	2.28, ddt (12.9, 9.1, 4.4)	2.10, m	2.08, ddt (13.7, 8.9, 3.9)
3	1.81, m; 1.53, m	1.49, m; 1.42, m	1.56, m; 1.46, m	1.57, m; 1.48, m
4	1.38, m; 1.24, m	1.41, m; 1.16, m	1.55, m; 1.18, m	1.47, m; 1.14, m
5	1.26, m; 1.24, m	1.43, m; 1.06, m	1.46, m; 1.21, m	1.46, m; 1.02, m
6	1.70, m	1.68, m	1.48, m; 1.48, m	1.37, m
7	1.53, m; 1.47, m	1.42, m; 1.41, m	1.36, m; 1.36, m	1.47, m; 1.31, m
8	1.68, m; 1.37, m	1.56, m; 1.49, m	1.36, m; 1.36, m	1.55, m; 1.46, m
9	3.63, m	3.62, m	3.62, m	3.62, m
10	1.54, m	1.53, m	1.55, m	1.55, m
11	1.47, m; 1.25, m	1.40, m; 1.31, m	1.56, m; 1.48, m	1.47, m; 1.41, m
12	1.47, m; 1.26, m	1.62, m; 1.35, m	1.62, m; 1.36, m	1.64, m; 1.34, m
13	3.35, m; 3.20, m	3.57, m; 2.95, ddd (13.4, 5.5, 2.9)	3.59, m; 2.98, ddd (13.4, 5.5, 2.8)	3.60, m; 2.96, ddd (13.6, 5.4, 2.8)
14	8.04, dd (5.9, 5.9)		8.05, dd (8.0, 2.8)	
15	1.62, m; 1.47, m	1.57, m; 1.53, m	1.61, m; 1.39, m	1.63, m; 1.33, m
16	0.90, t (7.5)	0.87, t (7.3)	0.87, t (7.2)	0.87, overlapped
17		1.08, d (6.9)	1.53, m; 1.39, m	1.57, m; 1.38, m
18			0.87, t (7.2)	0.87, overlapped
19	0.92, d (7.0)	0.91, d (6.7)		1.26, m; 1.26, m
20				0.87, overlapped
1′	4.86, d (1.5)	4.87, d (1.6)	4.87, s	4.87, d (0.9)
2′	3.56, m	3.55, m	3.55, m	3.57, m
3′	4.14, dd (3.0, 3.0)	4.15, dd (3.0, 3.0)	4.14, dd (3.0, 3.0)	4.15, dd (3.0, 3.0)
4′	3.56, m	3.55, m	3.55, m	3.57, m
5′	4.02, q (6.5)	4.03, q (6.5)	4.03, q (6.5)	4.03, q (6.5)
6′	1.21, d (6.5)	1.21, d (6.5)	1.21, d (6.5)	1.21, d (6.5)
8′	2.03, s	2.03, s	2.03, s	2.03, s

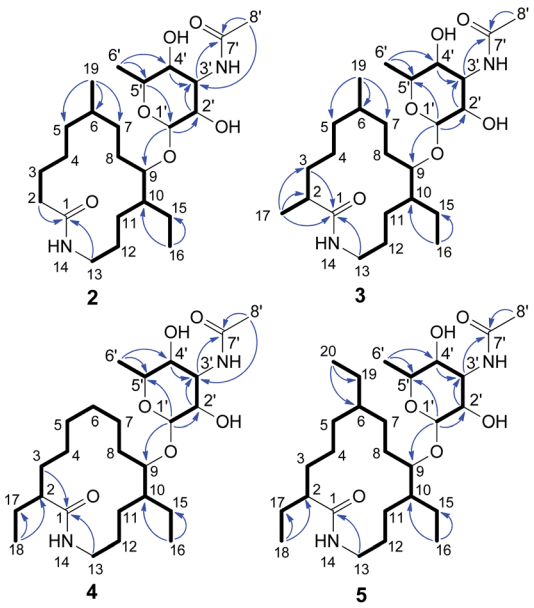

Fig. 3 Key ^{1}H–^{1}H COSY correlations (bold) and HMBC correlations (blue arrows) of **2–5**.

Fluvirucin B_8 (**3**) was isolated as an optically active powder. The HRESIMS gave a molecular formula of $C_{25}H_{46}N_2O_6$ (*m/z* 471.3444 $[M + H]^+$, calcd for 471.3434), which are 14 atomic mass units more than that of **2**. The ^{1}H and ^{13}C NMR spectroscopic data of **3** closely resembled those of **2**. The obvious difference was observed for the presence of one additional methyl (δ_H 1.08, d, J = 6.9 Hz, H_3-17; δ_C 18.9, C-17) in **3**. The COSY cross-peak of H_3-17/H-2 and HMBC correlations from H_3-17 to C-1 (δ_C 179.7, C), C-2 (δ_C 43.0, CH), and C-3 (δ_C 36.2, CH_2) allowed the assignment of the methyl group at C-2. Extensive analysis of 1D and 2D NMR spectra revealed that the rest part of **3** was the same as that of **2**. Therefore, the structure of **3** was determined as depicted.

Fluvirucin B_9 (**4**) was assigned a molecular formula as same as that of **3** on the basis of HRESIMS data. Comparison of ^{1}H and ^{13}C NMR spectra of **4** and **3** revealed a high similarity. The obvious difference was observed for the disappearance of one methyl and the presence of one more ethyl group in the ^{1}H spectrum of **4**. The methyl group of C-19 in **2** and **3** was replaced by a hydrogen, which led to a C-6 methylene. The ethyl group (δ_H 1.39, 1.53, H_2-17 and 0.87, t, J = 7.2 Hz, H_3-18; δ_C 27.7, CH_2, C-17 and 12.4, CH_3, C-18) was located at C-2 by interpretation of COSY cross-peaks of H_3-18/H_2-17/H-2 and HMBC correlations from H_3-18 to C-17 and C-2 (δ_C 50.9, CH). The remaining part was determined to be as same as that of **3** on the basis of comprehensive analysis of 2D NMR data. The structure of **4** was then deduced as shown.

Fluvirucin B_{10} (**5**), an optically active powder, possessed a molecular formula of $C_{27}H_{50}N_2O_6$ on the base of HRESIMS data at *m/z* 499.3763 $[M + H]^+$ (calcd for $C_{27}H_{51}N_2O_6$, 499.3747). The ^{1}H and ^{13}C NMR spectra of **5** was close to those of **4** with the exception of one more ethyl group (δ_H 1.26, H_2-19 and 0.87, H_3-20; δ_C 28.2, CH_2, C-19 and 12.8, CH_3, C-20). This is in consistent with the fact that molecular weight of **5** was 28 mass units more than that of **4**. The ethyl group was positioned at C-6 by COSY cross-peaks of H_3-20/H_2-19/H-6 and by HMBC correlations from

Table 3 *In vitro* antifungal activities of **1–5** (MIC_{80}, μg mL^{-1})

	Used alone			With 8 μg mL^{-1} of fluconazole	
Compounds	SC5314	901	904	901	904
1	>64	>64	>64	0.125	0.125
2	>64	>64	>64	>64	>64
3	>64	>64	>64	>64	>64
4	>64	>64	>64	0.125	0.125
5	>64	>64	>64	0.125	0.125
Fluconazole	0.125	>64	>64	>64	>64

H_3-20 to C-19 and C-6 (δ_C 39.8, CH). Cumulative analyses of the 1D and 2D NMR spectroscopic data allowed the structure assignment of **5**.

The relative configurations at C-2, C-6, C-9, and C-10 of aglycons in fluvirucins B_7–B_{10} could not be assigned independently on the basis of NMR spectroscopic data. Fluvirucins B_6–B_{10} are featured with a *N*-acetylated amino sugar in contrast to other fluvirucins. Specifically, fluvirucins B_6, B_9, and B_{10} are *N*-acetylated derivatives of B_1, B_0, and B_3/Sch 39185, respectively.[10,14,16,18] The NMR spectroscopic data of B_9 and B_{10} was compared with those of B_0 and B_3/Sch 39185. The ^{13}C NMR resonances of B_9 and B_0 showed a high similarity in aglycone part (Table S1†). Moreover, the negative optical rotation (OR) value of fluvirucin B_9 ($[\alpha]_D^{28.6}$ −29, *c* 1.0, MeOH) was close to that of B_0 ($[\alpha]_D^{28.6}$ −38, *c* 0.5, 1 : 1 MeOH/$CHCl_3$).[16] Meanwhile, the NMR and OR data of fluvirucin B_{10} ($[\alpha]_D^{30.9}$ −9.7, *c* 0.2, MeOH) were highly similar to those of fluvirucin B_3/Sch 39185 ($[\alpha]_D^{26}$ −5.8, *c* 0.5, MeOH).[10,14] All of fluvirucins have identical absolute configurations at C-2, C-6, C-9, and C-10, which were determined by X-ray crystallography for fluvirucins A_1 and B_1.[9,28] Fluvirucins B_7–B_{10} are likely to have the same configurations as known fluvirucins according to high similarity in NMR data of aglycon and OR values, and the assumed similar biogenetic pathway.

Antimicrobial activity

The isolated compounds were screened for antimicrobial activities against pathogenic bacteria including *Staphylococcus aureus* ATCC25923 and *Escherichia coli* ATCC25922, and *Candida albicans* (the standard clinical isolated strain SC5314, the fluconazole-resistant clinical isolates of 901 and 904).[29] Compounds **1–5** did not exhibit any activities against *S. aureus* and *E. coli* up to 128 μg mL^{-1} (Table S2†). Moreover, **1–5** were not active against *C. albicans* SC5314, 901, or 904 at 64 μg mL^{-1} (Table 3). However, when combined with 8 μg mL^{-1} of fluconazole, compounds **1**, **4**, **5** showed synergistic antifungal activities against fluconazole-resistant isolates of *C. albicans* 901 and 904 during 24 hours.

Discussion

Fluvirucins are characterized by 14-membered macrolactam attached with an aminosugar moiety. The structures of fluvirucins differ in the alkyl substituents and the sugar units. The alkyl substituents are usually located at C-2, C-6, and C-10, respectively, varying among methyl, ethyl, and hydroxyethyl groups (Fig. 4). The aminosugar, normally mycosamine or 4-*epi*-mycosamine, is appended to the macrocylic skeleton through a glycosidic linkage. According to the position of aminosugar attachment, fluvirucins are classified into "A" series having a sugar at C-3 (A_1, A_2) and "B" series with a sugar at C-9 (B_0–B_6).[10,21] Rarely, the aminosugar is *N*-substituted by a 2-phenethylaminocarbonyl group (B_4, B_5) or an acetyl group (B_6).[18] The aminosugar monosaccharide may also be replaced by disaccharide (Sch 42729) or trisaccharide (Sch 42282).[11,12] Besides, fluvirucins without any sugar unit (C_1, C_2) have been naturally isolated.[19] The discovery of fluvirucins B_7–B_{10} enriched the *N*-acetylated derivatives of fluvirucin.

Biosynthetically, fluvirucins belong to an uncommon class of polyketides (PKS) using a specific β-alanine as starter unit. Fluvirucins B_6–B_{10} share an ethyl group at C-10, but differ from each other in the alkyl substituents at C-2 and C-6. The alkyl substituents at both C-2 and C-6 vary between hydrogen atom, methyl, and ethyl groups which raises the question that the fluvirucin PKS may accept and process different substrates during chain extension. The biosynthetic gene clusters (BGC) for fluvirucins B_1 (*flu*) and B_2 (*flv*) have been completely identified and characterized.[30,31] The *flu* and *flv* show a high similarity between each other containing three modular PKS genes (*flu A–C* and *flv P1–P3*) and β-amino acid forming genes. The Flu A–C as well as the homologous proteins of Flv P1–P3 are both divided into five modules (M1–M5). The substrate specificity of acyl transferase (AT) in each module is experimentally examined, showing M2_AT and M4_AT specific for malony-CoA, M3_AT for methylmalonyl-CoA, and M1_AT and M5_AT for ethylmalonyl-CoA. We re-analyzed the AT domains in Flu A–C and Flv P1–P3 using bioinformatic tools (Fig. 5).[32,33] The M2_AT and M4_AT have the conserved "HAFH" motif (residues 194–197) that is specific to malonyl-CoA. Whereas, the M1_AT, M3_AT, and M5_AT have "VASH" or "YASH" motifs (residues 194–197), which are more specific for methylmalonyl-CoA (YASH motif) than ethylmalonyl-CoA (XAGH motif). The conserved motifs of AT domains could not explain the substrates promiscuity in fluvirucins. Probably, some residues dominating the canonical substrate specificity are not identified.

Fluvirucins are known to have antimicrobial and anthelmintic activities.[9,15,17,21] Compounds **1–5** displayed almost no antibacterial or antifungal activities when used alone at the tested concentrations. Decreased antimicrobial activity have been observed for other *N*-substituted fluvirucins or fluvirucins without aminosugar unit.[11,18–20] The current results implied that the aminosugar especially the free amino group in fluvirucins was essential for antimicrobial activity. The synergistic antifungal activities of **1**, **4**, and **5** against the fluconazole-resistant *C. albicans* suggested that fluvirucins may help fluconazole availability in the *C. albicans* cells by damaging cell wall or increasing intracellular fluconazole concentration, or targeting other proteins on a parallel pathway that converges on an essential process. Probably, the ethyl group at C-2 plays an important role in the synergistic antifungal activity.

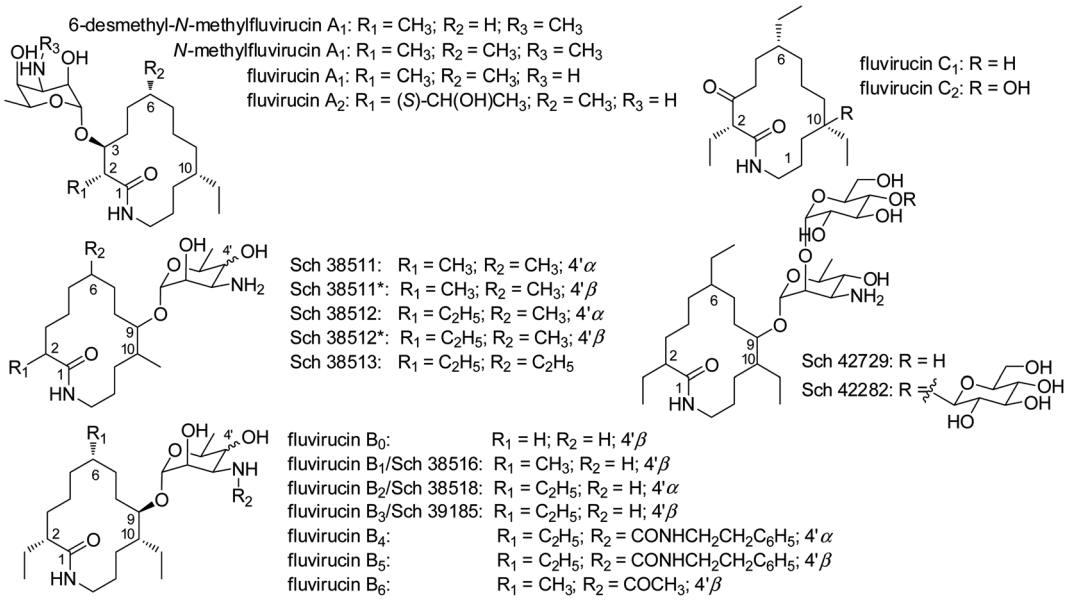

Fig. 4 Structures of known fluvirucins.

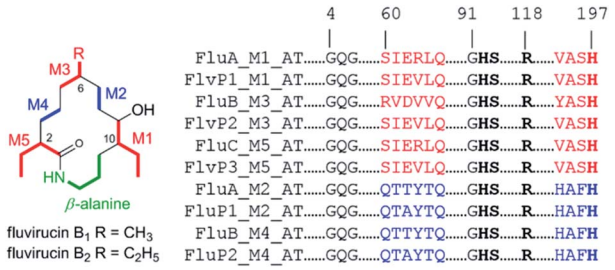

Fig. 5 Alignment of partial amino acid sequences of the AT domains of Flu PKSs (fluvirucin B_1) and Flv PKSs (fluvirucin B_2). Key catalytic residues are highlighted in bold, red for methylmalonyl-CoA or ethylmalonyl-CoA and blue for malonyl-CoA.

Conclusions

In summary, we have discovered fluvirucins B_7–B_{10} as new *N*-acetylated derivatives from a marine rare actinomycete. The results not only enrich the family of fluvirucin but also imply the substrates promiscuity of fluvirucin PKS. The biological results indicate the importance of free amino group of fluvirucins in the antimicrobial activity. The synergistic antifungal activity of fluvirucins with fluconazole is worthy of further investigation.

Experimental

General experimental procedures

Optical rotations were measured in MeOH on an Autopol-IV polarimeter at the sodium D line (589 nm). Infrared spectra were recorded in thin polymer film on a Nexus-470 FT-IR spectrophotometer (Nicolet, USA). The NMR spectra were recorded at 300 K on a Bruker AVANCE 600 NMR spectrometer. Chemical shifts are reported in parts per million (δ), with use of the residual CD_3OD signals ($\delta_H = 3.31$ ppm; $\delta_C = 49.0$ ppm) as internal standard, and coupling constants (J) are in Hz; assignments are supported by COSY, HSQC, HMBC, and NOESY experiments. High-resolution mass spectral data were obtained using a Bruker APEXIII 7.0 T FT-MS spectrometer in *m*/*z*, resolution 5000; an isopropyl alcohol solution of sodium iodide (2 mg mL^{-1}) was used as a reference. Semi-preparative HPLC was performed on an Agilent 1100 system with a UV detector using a YMC ODS-A column (5 μm, 250 × 10 mm). Silica gel (200–300 and 400–500 mesh; Yantai, China) was used for column chromatography. Precoated silica gel plates (HSGF254; Yantai, China) were used for TLC. Compounds were detected on TLC under UV light or by heating after spraying with anisaldehyde–sulfuric acid reagent. Antimicrobial activity assay was measured by a microplate reader SpectraMax M5.

Strain isolation and identification

Strain MYH522 was isolated by ISP2 medium (yeast extract 4.0 g, malt extract 10.0 g, dextrose 4.0 g, agar 20.0 g, distilled water 1.0 L, pH 7.2) from a marine sponge, which was collected off Xisha Island in South China Sea.

For phylogenetic study, strain MYH522 was grown in tryptic soy broth medium for 3 days at 28 °C. The 16S rDNA gene sequence was amplified by universal primers 27F (5′-AGTTTGATCMTGGCTCAG-3′) and 1492R (5′-GGTTACCTTGTTACGACTT-3′). PCR amplification reactions were prepared in a 25 μL reaction volume containing 12.5 μL of PCR 2× T5 Mix, 8.5 μL of distilled H_2O, 1 μL of 27F primer, 1 μL of 1492R primer, 1 μL DMSO, and 1 μL of DNA template, and was performed under reference conditions. PCR products were sent to the Sangon Biotech for sequencing. The 16S rDNA sequence was submitted to GenBank and blasted on NCBI. The multiple sequences were aligned by Clustal W. Phylogenetic trees were constructed with the MEGA7 software using neighbor-joining method. Bootstrap

analysis was used to evaluate the trees topology. Kimura two-parameter model was used for phylogeny construction and evolutionary distances analysis.

Fermentation, isolation, and structure characterization

The ISP2 medium was used for sporulation. Strain MYH522 was cultured with fermentation medium (starch soluble 10.0 g, yeast extract 4.0 g, peptone 2.0 g, $CaCO_3$ 1.0 g, $Fe_2(SO_4)_3 \cdot 4H_2O$ (8 g L^{-1}) 5.0 mL, KBr (20 g L^{-1}) 5.0 mL, distilled water 1.0 L, pH 7.0) at 28 °C for 7 days. An 18 L of fermentation broth was extracted with EtOAc for three times. The combined extracts were concentrated to afford a residue (1.54 g), which was subjected to ODS column chromatography, eluted by gradient MeOH–H_2O solution (30–100%, v/v) to yield 6 fractions (Fr. 1–6). Fr. 3 was separated by Sephadex LH-20 (MeOH/CH_2Cl_2, 1 : 2) to give 5 fractions (Fr. 3.1–3.5). Fr. 3.2 was subjected to semipreparative RP-HPLC (70% MeOH, 2.0 mL min^{-1}) to afford **2** (2.3 mg, t_R 15.6 min), **4** (14.9 mg, t_R 16.4 min), **3** (2.0 mg, t_R 18.5 min), **1** (65.5 mg, t_R 20.7 min), and **5** (6.5 mg, t_R 27.2 min), respectively.

Fluvirucin B_7 (2). White amorphous powder; R_f 0.28 (CH_2Cl_2/MeOH 15 : 1); $[\alpha]_D^{27.8}$ −76 (*c* 0.2, MeOH); IR (film) ν_{max} 3302, 2935, 2873, 1712, 1643, 1444, 1258, 981 cm^{-1}; ^1H and ^{13}C NMR spectroscopic data, see Tables 1 and 2; HRESIMS *m*/*z*: 457.3287 $[M + H]^+$ (calcd for $C_{24}H_{45}N_2O_6$, 457.3278).

Fluvirucin B_8 (3). White amorphous powder; R_f 0.30 (CH_2Cl_2/MeOH 15 : 1); $[\alpha]_D^{28.2}$ −29 (*c* 0.2, MeOH); IR (film) ν_{max} 3284, 2923, 2873, 1722, 1641, 1462, 1103, 979 cm^{-1}; ^1H and ^{13}C NMR spectroscopic data, see Tables 1 and 2; HRESIMS *m*/*z*: 471.3444 $[M + H]^+$ (calcd for $C_{25}H_{47}N_2O_6$, 471.3434).

Fluvirucin B_9 (4). White amorphous powder; R_f 0.30 (CH_2Cl_2/MeOH 15 : 1); $[\alpha]_D^{28.6}$ −29 (*c* 1.0, MeOH); IR (film) ν_{max} 3294, 2932, 1638, 1443, 1281,1102, 1017, 827 cm^{-1}; ^1H and ^{13}C NMR spectroscopic data, see Tables 1 and 2; HRESIMS *m*/*z*: 471.3449 $[M + H]^+$ (calcd for $C_{25}H_{47}N_2O_6$, 471.3434).

Fluvirucin B_{10} (5). White amorphous powder; R_f 0.33 (CH_2Cl_2/MeOH 15 : 1); $[\alpha]_D^{28.9}$ −9.7 (*c* 0.2, MeOH); IR (film) ν_{max} 3251, 2922, 1665, 1600, 1495, 1453, 1202, 702 cm^{-1}; ^1H and ^{13}C NMR spectroscopic data, see Tables 1 and 2; HRESIMS *m*/*z*: 499.3763 $[M + H]^+$ (calcd for $C_{27}H_{51}N_2O_6$, 499.3747).

Antibacterial activity assays

The antibacterial activity assays were performed against Gram-positive bacteria *S. aureus* and Gram-negative bacteria *E. coli* according to the Clinical and Laboratory Standards Institute (CLSI) methods.[34] The bacteria were grown in LB medium at 37 °C, 200 rpm for overnight, and were diluted to a concentration of 10^5 colony forming unit (CFU) mL^{-1}. Tested compounds and kanamycin in dimethyl sulfoxide (DMSO) were 2-fold serially diluted with LB medium to prepare 100 μL of solutions ranging from 128 to 4 μg mL^{-1}, and were added to 96-well microtiter plates with 100 μL of bacterial suspensions in each well. The plates were incubated at 37 °C for 24 h. Optical density was recorded at 630 nm using microplate reader. IC_{50} values refer the lowest concentration of compounds that cause 50% inhibition of bacterial growth.

Antifungal activity assays[29]

The antifungal activity assays was performed using a broth microdilution methodology adjusted from CLSI M38-A2 and M27-A3 standard. The fungal suspension was applied to 96-well plates at a concentration of 10^3 CFU mL^{-1} in RPMI 1640 medium. The tested compounds and fluconazole were serially diluted with final concentrations ranging from 64 to 0.125 μg mL^{-1}. To evaluate the synthetic effect, fluconazole was added into the fungal suspension at a concentration of 8 μg mL^{-1} before applied to 96-well plates, while the compounds were serially diluted. Plates were incubated for 24 hours at 30 °C. Optical density was measured at 630 nm with microplate reader, and background optical density was removed. The minimum inhibitory concentration (MIC_{80}) is that at which the growth of 80% tested strains is inhibited.

Author contributions

Conceptualization and supervision – P. S.; writing – H. Y. and P. S.; investigation and methodology – H. Y., S. C., H. L., and R. W.; review & editing – Y. J. and L. Y.; all authors have given approval to the final version of the manuscript.

Conflicts of interest

There are no conflicts to declare.

Acknowledgements

This research was funded by the National Natural Science Foundation of China (41876184, 81622044, and 82173867) and National Key Research and Development Program of China (2019YFC0312502 and 2019YFC0312601), Shanghai International Science and Technology Cooperation Project (21430713000), Shanghai Science and Technology Support Project in the Field of Biomedicine Project (19431901300), and Shanghai Pujiang Program (21PJD0081).

Notes and references

1 J. Bérdy, *J. Antibiot.*, 2005, **58**, 1–26.
2 W. Fenical and P. R. Jensen, *Nat. Chem. Biol.*, 2006, **2**, 666–673.
3 P. R. Jensen, B. S. Moore and W. Fenical, *Nat. Prod. Rep.*, 2015, **32**, 738–751.
4 P. Manivasagan, K.-H. Kang, K. Sivakumar, E. C. Y. Li-Chan, H.-M. Oh and S.-K. Kim, *Environ. Toxicol. Pharmacol.*, 2014, **38**, 172–188.
5 S. Qi, M. Gui, H. Li, C. Yu, H. Li, Z. Zeng and P. Sun, *Chem. Biodiversity*, 2020, **17**, e2000024.
6 R. Subramani and D. Sipkema, *Mar. Drugs*, 2019, **17**, 249.
7 K. Tiwari and R. K. Gupta, *Crit. Rev. Biotechnol.*, 2012, **32**, 108–132.
8 Z. Zhang, Y. Wang and J. Ruan, *Int. J. Syst. Bacteriol.*, 1998, **48**, 411–422.

9 V. R. Hegde, M. G. Patel, V. P. Gullo, A. K. Ganguly, O. Sarre, M. S. Puar and A. T. McPhail, *J. Am. Chem. Soc.*, 1990, **112**, 6403–6405.
10 N. Naruse, T. Tsuno, Y. Sawada, M. Konishi and T. Oki, *J. Antibiot.*, 1991, **44**, 741–755.
11 V. R. Hegde, M. G. Patel, V. P. Gullo, A. C. Horan, A. H. King, F. Gentile, G. H. Wagman, M. S. Puar and D. Loebenberg, *J. Antibiot.*, 1993, **46**, 1109–1115.
12 V. R. Hegde, M. G. Patel, A. C. Horan, A. H. King, F. Gentile, M. S. Puar and D. Loebenberg, *J. Antibiot.*, 1998, **51**, 464–670.
13 R. Cooper, I. Truumees, R. Yarborough, D. Loebenberg, J. Marquez, A. Horan, M. Patel, V. Gullo, M. Puar and B. Pramanik, *J. Antibiot.*, 1992, **45**, 633–638.
14 V. Hegde, M. Patel, A. Horan, V. Gullo, J. Marquez, I. Gunnarsson, F. Gentile, D. Loebenberg, A. King, M. Puar and B. Pramanik, *J. Antibiot.*, 1992, **45**, 624–632.
15 V. R. Hegde, M. G. Patel, V. P. Gullo and M. S. Puar, *J. Chem. Soc., Chem. Commun.*, 1991, 810–812.
16 S. Ayers, D. L. Zink, J. S. Powell, C. M. Brown, A. Grund, O. Genilloud, O. Salazar, D. Thompson and S. B. Singh, *J. Antibiot.*, 2008, **61**, 59–62.
17 S. Ayers, D. L. Zink, K. Mohn, J. S. Powell, C. M. Brown, T. Murphy, A. Grund, O. Genilloud, O. Salazar, D. Thompson and S. B. Singh, *J. Nat. Prod.*, 2007, **70**, 1371–1373.
18 A. S. Leutou, I. Yang, T. C. Le, D. Hahn, K. M. Lim, S. J. Nam and W. Fenical, *J. Antibiot.*, 2018, **71**, 609–612.
19 M. Costa, P. Zúñiga, A. M. Peñalver, M. Thorsteinsdottir, M. Pérez, L. M. Cañedo and C. Cuevas, *Nat. Prod. Commun.*, 2017, **12**, 679–682.
20 N. Naruse, O. Tenmyo, K. Kawano, K. Tomita, N. Ohgusa, T. Miyaki, M. Konishi and T. Oki, *J. Antibiot.*, 1991, **44**, 733–740.
21 K. Tomita, N. Oda, Y. Hoshino, N. Ohkusa and H. Chikazawa, *J. Antibiot.*, 1991, **44**, 940–948.
22 E. Llàcer, F. Urpí and J. Vilarrasa, *Org. Lett.*, 2009, **11**, 3198–3201.
23 Y. G. Suh, S. A. Kim, J. K. Jung, D. Y. Shin, K. H. Min, B. A. Koo and H. S. Kim, *Angew. Chem., Int. Ed. Engl.*, 1999, **38**, 3545–3547.
24 M. Martín, G. Mas, F. Urpí and J. Vilarrasa, *Angew. Chem., Int. Ed. Engl.*, 1999, **38**, 3086–3089.
25 P. Sun, F.-Y. Cai, G. Lauro, H. Tang, L. Su, H.-L. Wang, H. H. Li, A. Mándi, T. Kurtán, R. Riccio, G. Bifulco and W. Zhang, *J. Nat. Prod.*, 2019, **82**, 1264–1273.
26 J. Gong, P. Sun, N. Jiang, R. Riccio, G. Lauro, G. Bifulco, T.-J. Li, W. H. Gerwick and W. Zhang, *Org. Lett.*, 2014, **16**, 2224–2227.
27 P. Sun, D.-X. Xu, A. Mándi, T. Kurtán, T.-J. Li, B. Schulz and W. Zhang, *J. Org. Chem.*, 2013, **78**, 7030–7047.
28 N. Naruse, M. Konishi, T. Oki, Y. Inouye and H. Kakisawa, *J. Antibiot.*, 1991, **44**, 756–761.
29 H. Quan, Y. Y. Cao, Z. Xu, J. X. Zhao, P. H. Gao, X. F. Qin and Y. Y. Jiang, *Antimicrob. Agents Chemother.*, 2006, **50**, 1096–1099.
30 T. Y. Lin, L. S. Borketey, G. Prasad, S. A. Waters and N. A. Schnarr, *ACS Synth. Biol.*, 2013, **2**, 635–642.
31 A. Miyanaga, Y. Hayakawa, M. Numakura, J. Hashimoto, K. Teruya, T. Hirano, K. Shin-Ya, F. Kudo and T. Eguchi, *Biosci., Biotechnol., Biochem.*, 2016, **80**, 935–941.
32 F. Del Vecchio, H. Petkovic, S. G. Kendrew, L. Low, B. Wilkinson, R. Lill, J. Cortes, B. A. Rudd, J. Staunton and P. F. Leadlay, *J. Ind. Microbiol. Biotechnol.*, 2003, **30**, 489–494.
33 C. D. Reeves, S. Murli, G. W. Ashley, M. Piagentini, C. R. Hutchinson and R. McDaniel, *Biochemistry*, 2001, **40**, 15464–15470.
34 J. H. Rex and M. J. Ferraro, in *Methods for Dilution Antimicrobial Susceptibility Tests for Bacteria That Grow Aerobically; Approved Standard—Ninth Edition*, Clinical and Laboratory Standards Institute, Wayne, PA, 2012, vol. 32, 07–A0907–A0907–A09.